An experimental-theoretical study of the behaviour of hydrogen on the Si(001) surface

2000 J. Phys.: Condens. Matter 12 7655

(http://iopscience.iop.org/0953-8984/12/35/301)

J. Phys.: Condens. Matter **12** (2000) 7655–7670. Printed in the UK PII: S0953-8984(00)11815-6

An experimental–theoretical study of the behaviour of hydrogen on the Si(001) surface

D R Bowler†, J H G Owen‡, C M Goringe§, K Miki‖ and G A D Briggs
Department of Materials, Oxford University, Oxford OX1 3PH, UK
E-mail: david.bowler@ucl.ac.uk

Received 11 February 2000, in final form 5 June 2000

Abstract. An understanding of the dynamics of hydrogen on Si(001) is crucial to understanding gas-source growth, as the presence of hydrogen on the surface during gas-source growth of silicon and germanium dramatically changes the kinetics of growth and the morphology of the growth surface. We have used a combination of hot scanning tunnelling microscopy experiments and computational modelling, with the two techniques inter-relating, to investigate this system. By comparison with experimental and *ab initio* results, we have shown that our semi-empirical tight-binding code is sufficiently accurate to calculate diffusion barriers on the surface, while being efficient enough to be used in large simulations, such as that of the interaction of hydrogen with step edges. The behaviour of hydrogen has been investigated for diffusion along dimer rows, from one end of a dimer to the other, across dimer rows, down steps and away from a defect, with good agreement being found between measured and modelled diffusion barriers. We can now give a full account of the behaviour of hydrogen on the Si(001) surface.

1. Introduction

An understanding of diffusion processes at the atomic level is of great value scientifically, and hydrogen on Si(001) is a prototypical system for such studies. Furthermore, the system has many interesting properties, and is of great importance to the growth of silicon and germanium from gas sources such as silane (SiH_4) and germane (GeH_4). There have been previous experimental and theoretical studies of the hydrogen on Si(001), as an adsorbate, a passivant and a surfactant, and recently work on dynamical properties, though only on clean surface, and not near defects and steps.

Experimental studies have concentrated on the adsorption and desorption of monatomic¶ hydrogen [1–4], though recently Hill *et al* [5] applied the elegant atom-tracking technique [6,7] to diffusion along the dimer row and along the dimer bond. There have been several modelling studies of adsorption sites and the diffusion barriers along the dimer row, using a range of empirical and *ab initio* methods [8–13]. The major results of these studies relating to adsorption

† Present address: Department of Physics and Astronomy, University College London, Gower Street, London WC1E 6BT, UK
‡ Present address: HRL Laboratories, MS RL-62, 3011 Malibu Canyon Road, Malibu, CA 90265-4799, USA.
§ Present address: Key Centre for Microscopy and Microanalysis, Madsen Building (F09), University of Sydney, NSW 2006, Australia.
‖ Present address: Electrotechnical Laboratory, Tsukuba, Ibaraki 305-8568, Japan.
¶ The sticking probability of H_2 is almost zero on Si(001); almost all experiments crack H_2 to H before adsorption, although a subsequent precursor pairing mechanism may then operate [14].

0953-8984/00/357655+16$30.00

can be summarized as follows: the primary adsorption site is the dangling bonds of terrace dimers; at low coverages, single hydrogen atoms adsorb individually onto one end of a dimer; at higher coverages (i.e. above ∼0.1–0.2 ML [14]), two hydrogen atoms preferentially adsorb onto the same dimer. This pairing is energetically favourable by 0.2–0.4 eV [15].

In epitaxial growth of silicon and silicon–germanium there are substantial differences in the surface morphology according to the source of the silicon: an elemental source (SS-MBE) [16]; or from gas-source precursors such as silane or disilane (GS-MBE) [17, 18]. In the case of GS-MBE, surface hydrogen resulting from growth has three effects: it inhibits diffusion of the silicon, effectively increasing the diffusion barrier from 0.67 eV to 1.35 eV [19]; it saturates the step edges, favouring island growth over step-flow growth [18]; and it acts as a surfactant, e.g. inhibiting the segregation of germanium to the surface during Ge_xSi_{1-x} growth, so the 2-D wetting layer in Ge/Si(001) heteroepitaxy is much thicker [20]. Moreover, the saturation of step edges may provide a route for hydrogen desorption at a lower temperature than for terrace desorption [21].

The hot STM has made it possible to observe the motion of atoms directly at suitable temperatures (e.g. for H, 600–700 K). Our own previous work has studied single-atom diffusion at low coverages [22] and diffusion of pairs of hydrogen atoms on a saturated surface [23], using a combination of hot STM and theoretical modelling. There has been a more detailed STM study of dangling bond dynamics on the Si(001):D surface [24], which has come to much the same conclusions. The dangling bonds prefer to be paired, as had been predicted theoretically, and indeed the dangling bonds appear to diffuse as a pair at about 620–650 K. The atom-tracking, hot STM study [5] has measured directly the hopping barrier and attempt frequency for hydrogen diffusion along the dimer row and along the dimer bond.

In this paper, we describe the results of a comprehensive experimental–theoretical study of the behaviour of hydrogen on Si(001). We have used the diffusion of hydrogen along the Si(001) dimer rows at low coverage to validate the modelling against experiment, and also checked the semi-empirical modelling by comparison with *ab initio* calculations. We can now give a full description of the diffusion of hydrogen both on the clean surface (in all possible directions) and near defects and steps.

2. Experimental and theoretical methods

2.1. Experimental techniques

A JEOL JSTM-4500XT elevated-temperature STM was used, capable of operation up to 1500 K. The experimental methods are the same as those used in previous experiments to study the motion of individual hydrogen atoms [22]. The base pressure of the system during the experiment was 1.1×10^{-10} Torr (as measured by the mass spectrometer), the majority of which was due to hydrogen. The silicon wafers used were n-doped 0.1 Ω cm; they were cut into samples 1 mm by 7 mm and cleaned with a sulphuric acid/hydrogen peroxide etch. In UHV, they were cleaned by flashing to 1450 K. The sample was heated by direct current, and its temperature was measured using an infrared pyrometer which reads from 570 K to 880 K, with an accuracy of ±20 K. All images were taken using a tungsten tip, keeping the tunnelling current below 0.1 nA, and with sample bias voltages around +2 V to reduce interaction with the surface. The hydrogen dose was 99.99% H_2, with a small amount of water from the gas line, and was cracked by a hot tungsten filament located about 3 cm from the sample. The tip was mechanically withdrawn during dosing. After dosing, images were typically achieved within 5–15 minutes.

Great care was taken to ensure that there was no interaction between the tip and the adsorbed hydrogen. After dosing, if the sample was left for some time before an observation was made, the same results were obtained whether or not the tip had been scanning. The observations made were also independent of tip scanning direction, the scanning area and the bias used. These pieces of evidence lead us to believe that there was no influence of the tip on the sample (e.g. induced desorption).

All diffusion events measured correspond to 'tracer' diffusion, that is following particular atoms as they diffuse (this even applies to the high-coverage studies, which followed the 'motion' of vacancies on a saturated surface). Where there was a sufficient temperature range for observations (i.e. for the diffusion along the dimer row), the hopping barrier and attempt frequencies have been derived; however, this requires a large temperature range. For most of the events described in this paper, competing mechanisms prevented independent determination of attempt frequencies, which are therefore assumed (which is reasonable, given the uniformity of measured frequencies for different modes: $10^{13.78}$ Hz for the stretch mode, and $10^{13.26}$ Hz as for the bend mode [25, 26]).

2.2. Modelling techniques

We have used two modelling techniques to investigate the diffusion barriers: density functional theory (DFT), using both the local density approximation (LDA) [27, 28] and a generalized gradient approximation (GGA) [29]; and tight binding [30], using the linear scaling density matrix method (DMM) [31]. Calculations involving DFT are computationally more intensive than those involving the DMM, and can only be used on smaller supercells. Accordingly, the use of the tight-binding method and the accuracy of the parametrization used [32] have been validated against the DFT and experimental barriers (which are in extremely good agreement) and then used to study the larger systems. All DFT calculations used the plane-wave pseudopotential code, CASTEP [33], with non-local pseudopotentials of the Kerker type [34] in the Kleinman–Bylander form [35]. To calculate the shape of the diffusion barrier, an energy cut-off of 200 eV and a single special k-point at (0, 0.25, 0) were used; to verify that these are sufficient, the mid-point barrier height was recalculated using four special k-points (under the Monkhorst–Pack scheme), ultrasoft pseudopotentials and an energy cut-off of 250 eV. This confirmed that the original parameters give energy difference convergence. The unit cell used was two dimer rows wide, with two dimers in each row, and five layers deep. The bottom layer was constrained to remain in bulk-like positions, and terminated in hydrogen.

All tight-binding calculations used the real-space, linear scaling code DensEl [36], which is an implementation of the density matrix method of Li, Nunes and Vanderbilt [31]. The parametrization was designed specifically for the Si(001) surface and its interactions with hydrogen [32]. There is a problem with this parametrization, though it is one that can be corrected. When there is a long, weak bond between two atoms, physically there is little charge density between them, and there is a very slight attraction. In this tight-binding parametrization, the repulsive potential, which is used to represent electron–electron repulsion, is represented simply as a sum of pair terms; this is not proportional to the strength of the bond, and so with a long weak bond there is a net repulsion rather than the weak attraction expected physically (and seen in *ab initio* modelling). This has been investigated thoroughly, and can be compensated for by applying a correction to the barrier heights of 0.2 eV [32]. It also has an effect on the shape of reaction barriers, which is discussed below. The unit cells used were all ten layers of silicon deep, with the bottom five layers constrained to lie in bulk-like positions, and the final layer terminated in hydrogen.

The reaction barriers have been found using a simple method. In all cases presented in this paper, it was easy to find an unambiguous reaction coordinate: a line in real space from the start to the end position. The diffusing hydrogen was constrained to lie in a given plane normal to the reaction coordinate, and the energy was minimized with respect to the other atomic coordinates; a series of these minimizations were carried out with the plane at different positions along the diffusion path. This method, which is computationally efficient, allowed a simple determination of the energy barrier. The problem with the calculation of reaction barriers with the tight-binding parametrization shows itself when the energy is plotted. Figure 1(a) shows the barrier calculated using LDA, and displays the classic rounded peak to the curve, indicating a well-defined second derivative. Figure 1(b), however, shows that the barrier calculated using tight binding appears to have a cusp at the peak. Normally, this is an indication that the reaction coordinate chosen is incorrect; here, however, it is an artefact caused by the anomalous repulsion at long bond lengths (described above and in more detail in [32]). The reaction coordinate chosen is the same as that for the LDA calculation, which shows correct behaviour; furthermore, the derivative of the tight-binding curve is continuous, and is in fairly good agreement with the derivative of the DFT curve. The barrier heights calculated using tight binding are also in extremely good agreement with experimental results where available (after the correction discussed in [32]). From these pieces of information, we conclude that the corrected barriers calculated using tight binding are valid, but that the detailed shape is incorrect, due to the anomalous repulsion found. Rather than display graphs which appear to have an anomalous cusp (and might cause confusion) we shall simply quote the barrier heights.

3. Results and discussion

3.1. STM imaging of adsorbed hydrogen

Hydrogen adsorbs onto the Si(001) surface by inserting into the π-bond of the silicon dimers and reacting with the dangling bond on one of the two silicon atoms. The remaining half-filled dangling bond appears as a bright blob in the STM; an example of this can be seen in figure 2(a). Hydrogen adsorbs randomly at coverages below 0.1 ML [3], but above this limit, it preferentially pairs up onto a single silicon dimer [14,15]. This paired configuration, known as a monohydride dimer, with one hydrogen atom adsorbed onto each end of a silicon dimer and the σ-bond intact, is the most stable structure for hydrogen adsorption below 1 ML. The Si–H bonds lie well below the Fermi level and appear dark in the STM compared to the clean dimers. The apparent height difference between a clean dimer and a monohydride dimer changes with the bias voltage from 0.7 Å at -3 V, to as much as 2 Å at -1.5 V [17].

In high-coverage images of the surface, these monohydride dimers form the background (figure 2(b)). The bright foreground features in figure 2(b) are clean dimers (circled), which are resolved into a distinctive double-lobed blob (indicative of the anti-bonding π^*-orbital) in empty-states images. In this image, the hydrogenated dimers are resolved into pairs of dark dots, and the image of a clean dimer is much larger than the dimer from which it springs. Isolated monohydride dimers appear very similar to single-missing-dimer defects (1-DV) at normal imaging voltages ($\sim$1.5–2 V). They may be distinguished from such defects at large bias voltages [17]. We have found that they may also be distinguished at low sample bias: the dimers next to a 1-DV exhibit an enhanced contrast at low bias voltages [37], whereas the dimers next to a monohydride dimer are unaffected, enabling the two to be distinguished; this is illustrated in figure 3.

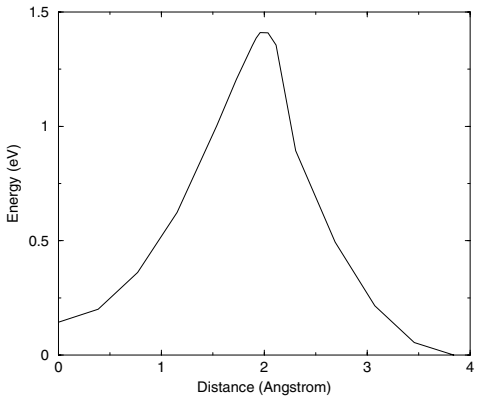

(a)

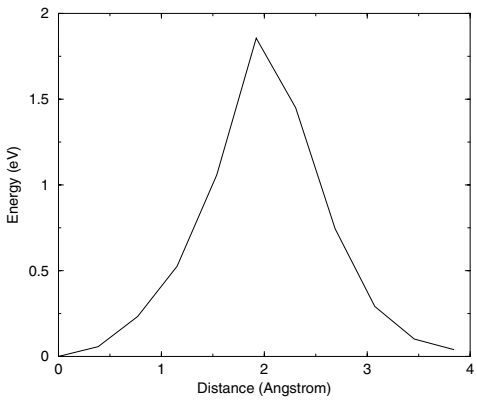

(b)

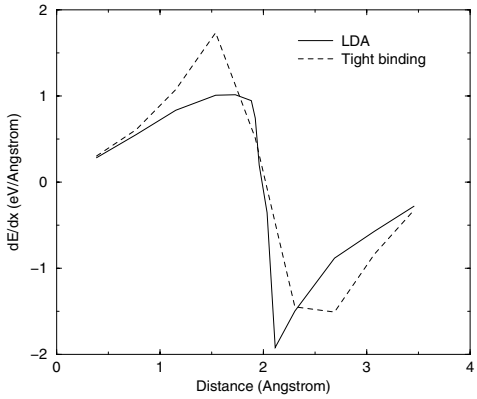

(c)

Figure 1. Modelling barriers of single-atom diffusion. The DFT results are shown in (a). LDA gives a barrier of 1.41 eV, but correction with the GGA with spin raises this barrier to 1.65 eV, which agrees well with the experimental barrier within errors. The TB result is shown in (b). The barrier here is 1.85 eV. The corrected value of 1.65 eV is well within experimental uncertainty. (c) The differentials of the curves in (a) and (b), showing that the tight-binding results are following the correct behaviour, and only form a cusp at the mid-point because of the anomalous repulsion discussed in the text.

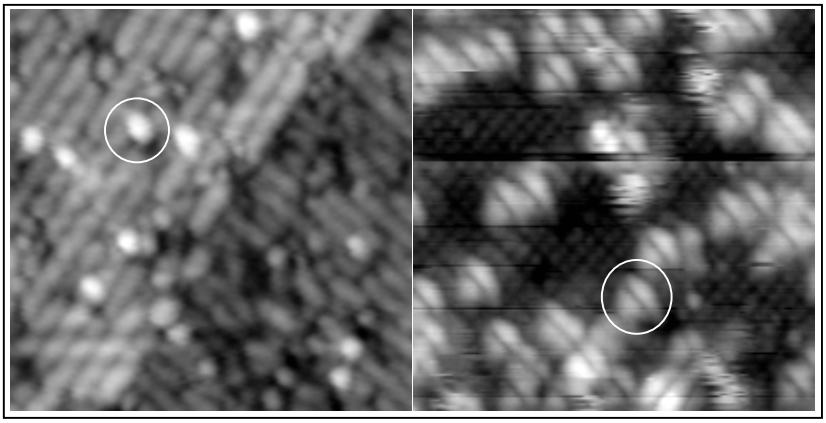

(a) (b)

Figure 2. Adsorbed hydrogen. (a) Low coverage. In this regime (<0.1 ML), hydrogen adsorbs at one end of a dimer, which becomes dark. The energy of the orbital at the clean end of the dimer shifts upward, and so it appears bright. One of these bright dots is indicated with a circle. (b) High coverage. Here, hydrogen adsorbs onto both ends of the dimer to form a monohydride dimer. These can be seen as dark rows of dots in the background. A clean dimer, which may be thought of as a vacancy in the hydrogen layer, appears bright relative to the background (circled).

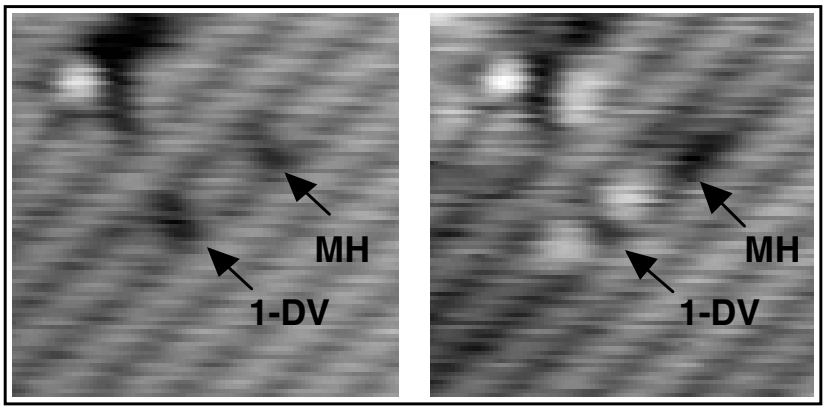

(a) (b)

Figure 3. An image of the Si(001) surface with a small exposure of disilane, (a) at −2 V and (b) at 1 V. A 1-DV and a monohydride dimer are marked with arrows. In (a) they appear identical, while in (b), the 1-DV shows an enhancement around it.

3.2. Diffusion on perfect terraces

The Si(001) surface is highly anisotropic, and contains many features such as missing-dimer defects and steps. It is important to understand the behaviour of hydrogen on the perfect surface before considering the effect of such features. There are three different directions in which a hydrogen atom adsorbed onto one end of a terrace dimer may hop in order to reach an equivalent site. These are shown schematically in figure 4. The closest site, with the lowest barrier to diffusion, is the empty dangling bond at the other end of the silicon dimer (a). The next closest site is the next dimer within the same dimer row (b). Lastly, the hydrogen atom may hop across dimer rows onto the next dimer row (c), though this hopping is rarely seen. The

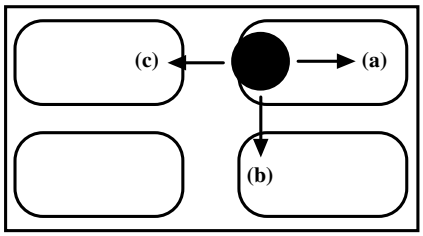

Figure 4. The possible pathways for a diffusing hydrogen atom. The hydrogen atom can hop to the other end of the dimer (a), to another dimer in the same row (b) or to a dimer in an adjacent row (c).

situation becomes more complex if the hydrogen coverage is high (i.e. site (a) is occupied) or if a step or defect are present; these situations are dealt with below in sections 3.2.4, 3.3.1 and 3.3.2. In our previous work, inter-dimer diffusion (hopping to site (b) in figure 4) was the subject of a detailed study using STM, and both DFT and tight-binding methods. Subsequent to that work, a tight-binding parametrization has been created specifically for the Si(001)–H system, and new values for the diffusion barrier have been calculated. Our results demonstrate that the tight-binding method is more than adequate to describe diffusion barriers in this case, and thus we have used it with confidence to obtain values for other diffusion barriers in situations where the unit cells required would make a DFT calculation prohibitive. After reviewing diffusion along the dimer row, we shall describe the other simple diffusion cases (hopping to sites (a) and (c) in figure 4), and then move on to more complex situations: diffusion of pairs of hydrogen atoms, and diffusion across defects and step edges.

3.2.1. Diffusion along dimer rows. The diffusion of hydrogen atoms along the dimer rows (inter-dimer diffusion) is the major mechanism for long-range diffusion across the terraces. For this reason, it was investigated most thoroughly [22], with observations of diffusion taken across a wide temperature range (200 K), in order to obtain accurate values for the activation barrier and the prefactor. The barrier which was obtained in that work was 1.68 eV. The temperature error ($\pm$20 K) is the major source of uncertainty in these data, giving an error in the measured barrier of $\pm$0.15 eV [22]. This is in good agreement with recent measurements [5], which find a value of 1.75 ± 0.1 eV. However, the determination of the diffusion barrier of hydrogen on silicon is not only important for experimental studies, but is also an important touchstone for the accuracy of modelling calculations. Although the experimental value is not without uncertainty, we may conclude that the value of 1.3 eV obtained using DFT with the LDA [9], and the value of 2.0 eV obtained using CI (configuration interaction) calculations without substrate relaxation [10] are both outside the range of uncertainty. Inclusion of substrate relaxations (using an empirical Stillinger–Weber potential) into the CI calculation gives a value of 1.65 eV, consistent with our experimental result. A recently developed empirical potential [13] yields a barrier of 1.8 eV, which is maybe a little high, but within experimental error. For our own calculations, we have used DFT with the LDA and GGA (which can be more accurate for reaction barriers) for comparison, also accounting for spin at the start and mid-point.

In our previous work, we obtained barriers of 1.20 eV and 1.51 eV respectively. By performing the calculation with improved convergence (i.e. higher plane-wave cut-off and more k-points), and using more points on the diffusion path, we have achieved values which are more in agreement with our experimental value. A plot of the barrier given by the calculations using LDA is given in figure 1(a). The LDA, which is known to overbind, gives a value of

1.39 eV, while the GGA gives a value of 1.55 eV. Performing a spin-polarized calculation increases the GGA barrier to 1.65 eV, which is well within experimental uncertainty. A plot of the barrier calculated with tight binding is shown in figure 1(b) (its anomalous shape has been discussed in section 2.2). After applying the correction described section 2.2, the barrier found is 1.65 eV $\pm$ 0.20 eV, which is in excellent agreement with both the experimental and DFT values. Having shown that the energy barriers calculated using tight binding are in agreement with both experimental and *ab initio* calculations, we will proceed in the following sections to use tight-binding calculations of energy barriers for other important diffusion processes.

3.2.2. Intra-dimer hopping. Below the temperature at which the hydrogen atoms are able to pair up, they are still able to hop from one end of the dimer to the other. By the time the atoms are diffusing along dimer rows, this motion happens too fast to detect, and the blobs become fuzzy and symmetric with respect to the underlying dimers [22]. Figure 5 shows a small coverage of hydrogen atoms (8% ML) at a surface temperature of 450 K. The white dots result from single, unpaired hydrogen atoms. The larger blobs are thought to be the effect of several hydrogen atoms on neighbouring dimers blurred together by the STM tip. There is experimental and theoretical evidence for interaction between the orbitals on neighbouring atoms [15, 24]. The fact that so few are paired, despite the large density of white dots, demonstrates that the hydrogen is unable to hop from dimer to dimer at this temperature. However, by comparing the positions of white dots in a series of images of the same part of the surface, we are able to see that many of the white dots are moving from end to end of the dimers. Two examples are circled in figure 5 [38]. By counting the motions of these atoms, we find that the hopping probability is 10^{-2} s^{-1} at this temperature, which corresponds to a barrier of 1.4 $\pm$ 0.2 eV for a prefactor of 10^{13} s^{-1}. Other work has found that intra-dimer hopping is completely suppressed below 500 K [24], which would correspond to a rather higher barrier (however, in that study, deuterium was used, which will have an effect upon the kinetics). The recent hot STM atom-tracking study [5] found a barrier of 1.01 $\pm$ 0.05 eV, with an attempt frequency of $10^{10.3\pm0.5}$ Hz; this rather low attempt frequency is unusual, and requires further investigation. It is worth noting that if an attempt frequency of 10^{13} Hz were assumed, the

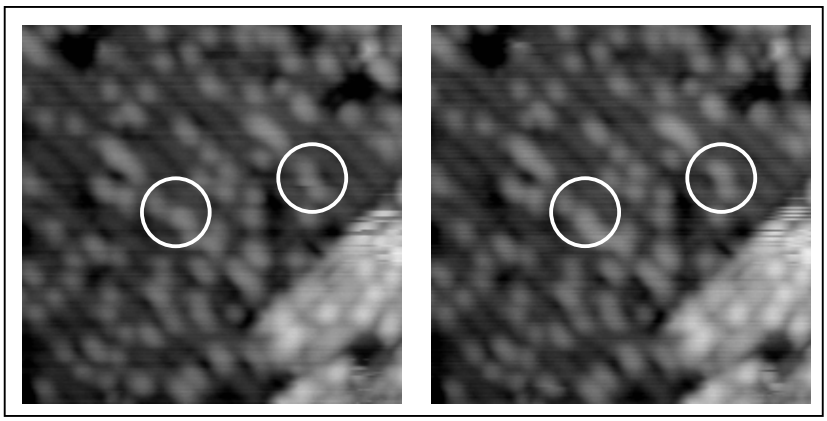

Figure 5. 430 K, 12 nm square, −1.3 V, 0.08 nA. At this temperature the hydrogen atoms are unable to pair, but can move from one end of the dimer to the other. Two examples of moving dimers are shown. More become apparent when a sequence of images are animated. This motion has an estimated barrier from experiment of 1.4 eV.

barrier would be 1.4 eV. The recent empirical potential study [13] found a barrier of 1.1 eV, but was not able to account for the buckling of the dimers on the surface which may have an effect on the barrier.

This process has been modelled using our tight-binding parametrization. The unit cell was two dimer rows wide and six dimers long, with the usual depth and termination. The hydrogen was forced to remain in planes of constant x (i.e. along the dimer). The corrected barrier for this reaction is 1.44 ± 0.20 eV, which agrees with the available experimental data (for an attempt frequency of 10^{13} Hz—but is a little high for lower attempt frequencies; clarification of the unusually low attempt frequency [5] is required). From this, we can conclude that the blurring of the white dots seen at 600 K and above is due to rapid intra-dimer hopping.

3.2.3. Diffusion across dimer rows. We have a few pictures where the hydrogen is forming 'fluxional' features, and this streak or smudge crosses the dimer rows. The diffusion of hydrogen across dimer rows is impossible to measure, as the atom, once it has hopped across, will diffuse away extremely fast along the dimer row, and so instances are rarely seen. In figure 6, a single hydrogen atom is trapped between two missing-dimer defects. Later, it has disappeared, indicating that slow diffusion across dimer rows is possible at a temperature of

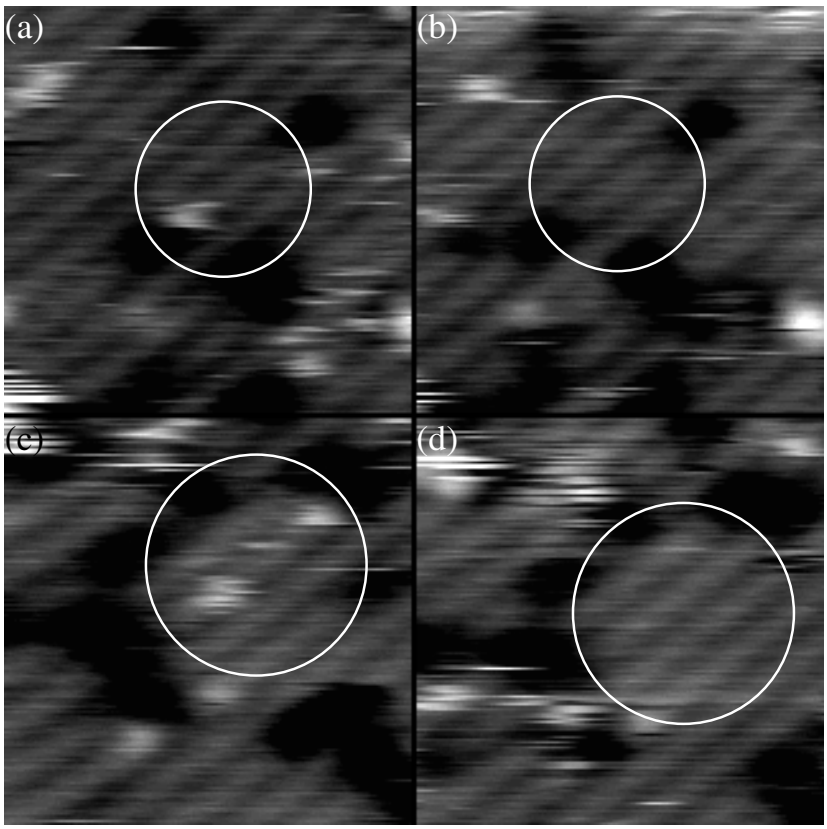

Figure 6. 8 nm square, −1.2 V, 0.08 nA, 700 K, 5 s between pictures. In these pictures, a hydrogen atom is trapped between two defects (a). It is no longer present in the second image (b). Similarly, for (c) and (d). Diffusion across the dimer rows has therefore probably occurred.

700 K. The lifetime of the atoms in these images is of the order of a few hundred seconds, which implies that the barrier is about 2.1 eV (lower and upper limits of 1.9 eV and 2.4 eV can be estimated from the range of lifetimes (100–2000 s) and attempt frequencies (10^{12}–10^{14} s^{-1})). While the barrier cannot be determined reliably by experimental means, it can be investigated using tight binding. The unit cell used was, as above, two dimer rows wide, and six dimers long. The hydrogen was again forced to remain in planes of constant x (across the trench between dimer rows). The energy for the diffusion gave a corrected barrier of 2.38 ± 0.20 eV, which is perhaps a little high, but does explain the confinement of hydrogen to individual dimer rows at temperatures below 700 K.

3.2.4. Hopping of paired dimers. During gas-source MBE growth, the coverage of hydrogen is high, and it will be paired up on dimers in the surface; it is thus necessary to understand diffusion in this situation as well. Paired hydrogen has an increased stability compared to single hydrogen atoms, and hence there is an increased barrier to diffusion [23]. As shown in figure 2(b), the prominent features of an STM image of Si(001) at high hydrogen coverage are due to the few dimers which have no hydrogen on them. It is the change in position of these clean dimers, as a result of the adsorbed hydrogen moving from dimer to dimer, that may be measured by the STM. This is analogous to the diffusion of vacancies in the bulk, and it is convenient to discuss the motion of these dangling bonds, rather than the hydrogen atoms.

At around 600–620 K, all the dangling bonds are paired, and there is the appearance of concerted motion of a clean dimer from one site to the next [23, 24]. As the temperature is raised, there is an increasing tendency for the dangling bonds to unpair, and a 'fluxional' feature is formed [24]. These features are long streaks along a dimer row, similar to that seen at low coverage [22], and silicon dimer diffusion [6]. These 'fluxional' features eventually pair up, to form a clean dimer once more [24]. A series of images of the saturated surface at 650 K is shown in figure 7 [38], which observations confirm those of [24]. In many cases, the clean dimer is stationary while being imaged, but its position changes between images (examples are indicated by A and B in the pictures). In other instances, streaky features several dimers long are seen (an instance is indicated by C). Over the course of a few frames, a clean dimer may become a streak, and then go back to being a clean dimer again in a different position on the surface, so we may be sure that these streaks are the images of highly mobile hydrogen atoms.

Compared to diffusion of single atoms on the clean Si(001) surface, the saturated surface diffusion events are happening quite slowly: the observed hopping rate of the clean dimers at 650 K is about 10^{-2} hops s^{-1} parallel to the dimer rows, while at low coverages, single hydrogen atoms are moving at about 20 hops s^{-1} along the dimer rows at this temperature. Since each 'diffusion event' requires the motion of two dangling bonds (or equivalently, two hydrogen atoms), we cannot obtain an activation barrier directly from this observed hopping rate. To throw some light on possible diffusion mechanisms, we have performed tight-binding (TB) diffusion calculations. In these calculations, the unit cell was one dimer wide, and six dimers long. One of the six dimers in the unit cell was clean, and the other five were saturated with hydrogen. In the first calculation, the two hydrogen atoms were forced to diffuse together (both atoms were constrained to remain in a plane of constant y, along the dimer row), and were dragged along the dimer row in concert. This procedure is indicated schematically in figure 8(a). In the second calculation, first one hydrogen was forced to diffuse, and then the other (i.e. the constraint was applied to each hydrogen consecutively). This is shown in figures 8(b) and 8(c). The corrected energy barriers for these calculations were 3.2 ± 0.15 eV for simultaneous diffusion, and in the case of sequential diffusion, 1.98 ± 0.15 eV for the first diffusion event, and 1.69 ± 0.15 eV for the second. The energy cost for the first hydrogen of a pair to diffuse is higher than that of a single atom, as it requires the breaking up of a π-bond

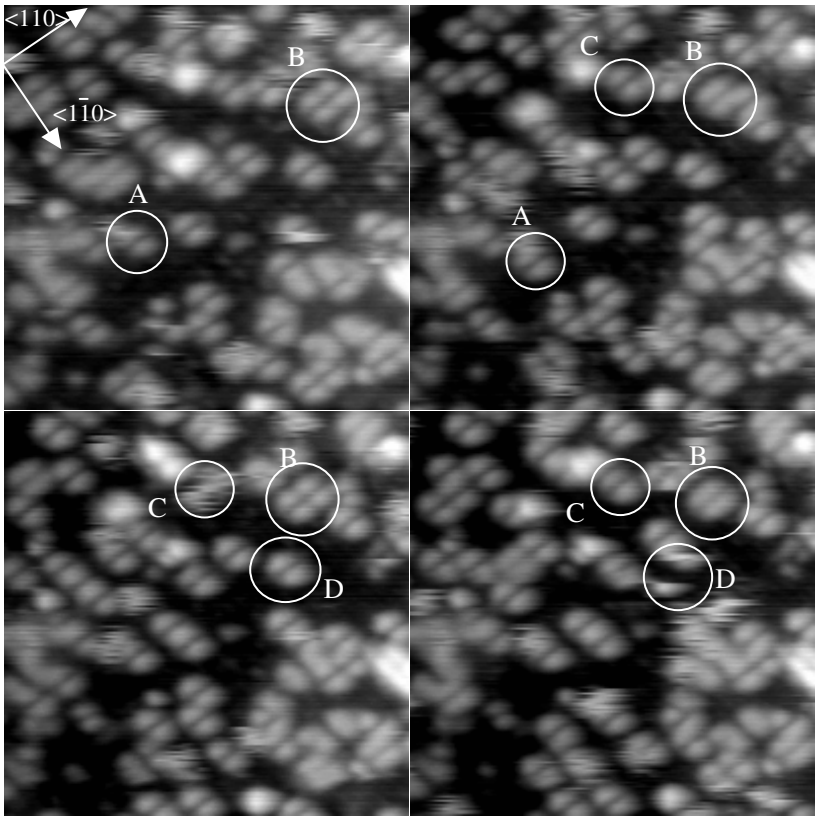

Figure 7. 14 nm wide, +1.5 V, 0.08 nA, 640 K, 18 s/picture. Four sequential frames from a 'movie' are shown (reading from left to right). Examples of moving vacancies are shown in each case: a rare case of a dimer diffusing across a dimer row (A); a group of clean dimers joining, splitting up and then rejoining each other by diffusion (B); and a dimer becoming a streak and then reverting to a dimer (C). In D, a dimer becomes two brighter dots, at opposite ends of a row. This may be an example of the situation in figure 8(d).

on the destination dimer without restoring that on the initial dimer (as is the case in diffusion of a single hydrogen). This leads to an increased barrier and hence an increased temperature at which it first occurs. However, once it has hopped, the probability for the second hydrogen to hop on (or, equivalently, for the first to hop back) is greatly reduced; at 700 K this will be about 150 times more likely to happen than for the first hydrogen to hop. These results make the mechanism clear: the rate-limiting step is the breaking up of the paired hydrogen, which is then followed extremely quickly by regrouping, with a 50% probability that the position of the clean dimer will have moved one site. Thus, at an experimental temperature where the vacancies are observed to be hopping every ten seconds or so (i.e. once per image on average) the mean hopping time for the first atom will be ten seconds, while for the second it will be every 1/20th of a second (i.e. the timescale of a linescan), leading to the appearance of concerted vacancy motion in the STM. Determination of the rate-limiting step enables us to estimate an activation barrier from our experimental observations [23]. For the above hopping rate (10^{-2} s^{-1}), the activation barrier along the dimer rows is 1.96 eV with a prefactor of 10^{13} s^{-1}. This is 0.28 eV higher than the measured activation barrier for single-atom diffusion (1.68 eV), using the same prefactor [22], and is in good agreement with the difference in our

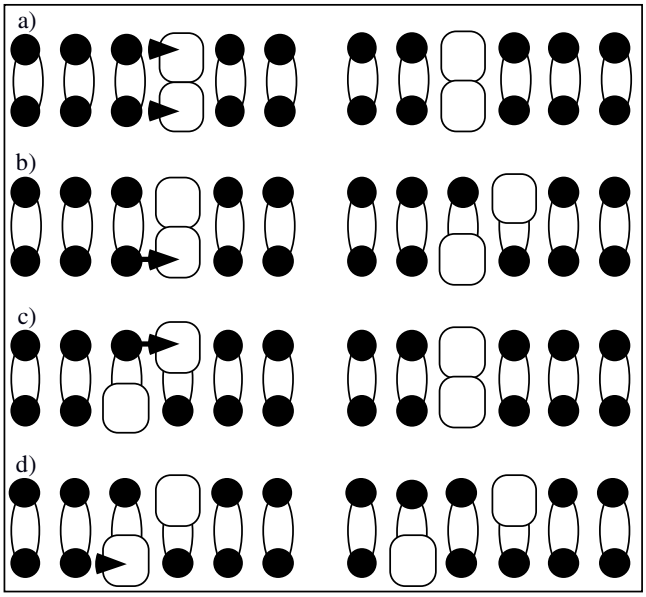

Figure 8. A schematic diagram of the diffusion of pairs of hydrogen atoms. In (a), the two atoms move simultaneously. This has an extremely high barrier (3.2 eV). A lower barrier (1.98 eV) is obtained if one of the pair moves first, leaving the two hydrogen atoms in an unstable, unpaired state (b). Then several things can happen. They can pair up again (c). Or, much less likely, the hydrogen may move so as to leave the two unpaired atoms isolated and unable to pair up again (d). Situations which may correspond to (c) and (d) are seen in figure 7.

tight-binding calculations (where the corrected barriers are 1.98 eV and 1.65 eV, yielding a difference of 0.33 eV).

With this mechanism we can also explain the conversion of the stable clean dimers into the 'fluxional' features [24] which are observed (C in figure 7). In the diffusion process described above, first one of the two atoms hops onto the clean dimer (figure 8(b)). This is an unstable state, and the next move is for the two unpaired hydrogen atoms to hop back together again. The vacancy will then have moved either zero or one dimers (figure 8(c)). An alternative possibility, however, is for an atom to hop from a third dimer onto one of the unpaired dimers, which would leave two unpaired dimers separated by a paired dimer (figure 8(d)). Although this is a higher-energy state, the two unpaired hydrogen atoms are prevented from pairing up by the dimer in between them. In this situation, the two hydrogen atoms will be able to oscillate back and forth extremely fast from one end to the other of the dimer, and between dimers more slowly, until the right combinations of motions allows the two hydrogen atoms to pair up again. The observation of 'fluxional' features (at high coverage) at a similar temperature to 'smudges' (at low coverage) indicates that the barrier to diffusion of a lone H atom on the saturated surface is similar to the barrier on a clean surface. The incidence of these features increases with temperature, which would follow naturally from the increase in entropy of two unpaired dangling bonds against a single pair of dangling bonds.

3.3. Diffusion at defects and surface steps

On a real surface, there are typically a few per cent of missing-dimer defects in the terraces (figure 2(a)). They will present a barrier to the diffusion of a hydrogen atom along the dimer

row, and may therefore control terrace diffusion on a real surface. Furthermore, it has been suggested that the dangling bonds present in defects and at step edges play a major role in hydrogen desorption processes [12] and therefore we have studied the stability of atoms adsorbed on the bonds, and also the barriers to diffusion onto these sites.

Two further pieces of experimental evidence have prompted a detailed computational investigation of the interaction of hydrogen with step edges. First, a study of hydrogen desorption from vicinal Si(001) miscut surfaces found that there was a change in the desorption kinetics with the angle of miscut [21]. This suggests that the step-edge site is a favourable place for desorption. Second, in our studies of the growth of Si(001) using disilane, we found that at a temperature of 650 K, island nucleation was seen close to the B-type step edges [18]. Such a step edge acts as a sink for surface-diffusing silicon atoms, and a denuded zone would be expected close to it, within which impinging silicon atoms would adsorb at the step edge before encountering another atom and forming an island. The best explanation for the presence of islands so close to the step is that the B-type step edges are saturated with hydrogen, passivating the normally active adsorption site. However, there was no change in the STM contrast of the B-type steps even when we had good evidence that hydrogen was present, so this cannot be confirmed experimentally. A theoretical investigation is therefore invaluable to test this hypothesis, though there is strong experimental evidence to back it up.

3.3.1. Adsorption and diffusion at defects. In figure 6, two pairs of images taken at 650 K of a short strip of a dimer row terminated in missing-dimer defects are shown. The images in each pair were taken ten seconds apart. The white streaky features seen in (a) and (c) are due to a single hydrogen atom that is trapped between the two defects (the coverage here is around 5% ML). In (a), it appears to be trapped on the end dimer, so it cannot move as the tip scans over it. In (c), the white dot is broken up into several streaks. In each case, the hydrogen atom has disappeared in the subsequent image ((b) and (d) respectively), indicating that this may be a rare observation of diffusion across the dimer row. The pinning of the atom in (a), where diffusion would normally be extremely rapid, indicates that the barrier to diffusing off this end dimer is higher than for a dimer on an infinite terrace.

Modelling of the adsorption energy of hydrogen onto the dimer next to the defect showed no significant difference compared to the case for a standard dimer. However, modelling of the barrier to the escape of a hydrogen atom from this end dimer onto the next dimer found that the corrected barrier is 2.35 eV $\pm$ 0.20 eV, which is 0.7 eV higher than the barrier to inter-dimer diffusion on the clean surface. (The modelling was performed in a unit cell which was six dimers long and two dimer rows wide, with a single missing dimer in one row.) The explanation for this large increase in the barrier is the strain induced in the dimer by the presence of the defect. The defect pulls the dimers on either side towards each other, and also flattens the buckling angle of the dimers to about 3° (from about 15°). These two effects combine to lengthen the gap between the edge dimer and its neighbour, which in turn leads to an increased barrier. Thus a hydrogen atom which adsorbs onto one of these sites is likely to stay there, while an atom approaching a defect will be reflected by the large activation barrier, so the defect is acting as a fence. It also explains the phenomenon in figure 6, where the hydrogen was trapped between two fences, and finally escaped by diffusing across dimer rows. (This will occur more often than diffusion into a defect, even though the barriers for these two processes are similar, since the defect is only encountered at the ends of a string of dimers.) The distortion of the dimer next to a defect is very similar to that of the dimer at the top of a B-type step, with a similar effect, as we shall see in the next section. These defects block the fast diffusion along the dimer row, and prevent isolated H atoms from pairing up.

3.3.2. Adsorption and diffusion at step edges. We set out to answer two questions concerning the interaction of hydrogen and the B-type step edge: is the step a favourable adsorption site, and is the barrier to diffusion of hydrogen off the step greater than that on the clean surface? The rebonded B-type step edge has dangling bonds at the base of the step. By analogy with singly adsorbed hydrogen atoms on the terrace which find it preferable to pair up, these sites should be favourable adsorption sites.

The energies of adsorption on the terrace, and at the top and bottom of a step were modelled (the sites are indicated schematically in figure 9). We found that an isolated pair of hydrogen atoms at the base of the step are favoured by 0.13 eV/pair, while a completely saturated step is favoured by 0.16 eV/pair compared to a pair on the clean terrace; these numbers compare well to those measured (0.2 eV) [39] and calculated (0.12 eV) [40] for double-height steps. A pair of H atoms on the dimer at the top of the step is disfavoured by 0.06 eV, although this figure is within the error of the calculation. We have also investigated the barriers to diffusion down the step itself, from the dimer at the top of the step to the dangling bond at the base of the step. Diffusion down the step was modelled using a unit cell with five dimers in the upper terrace, and the equivalent of five in the lower (this is the smallest unit cell for a rebonded step which ensures that there are no interactions between steps [41]). The barrier is found to be 1.37 eV after correction. The low barrier is caused by the geometry of the system, as the local environment is quite similar to the pathway for hopping from one end of a dimer to the other. This means that the hydrogen atom is able to remain bonded to both silicon atoms, unlike inter-dimer diffusion where the hydrogen is only bonded to one atom, and the mid-point is highly unstable. The barrier to diffusion up or down the step is 0.3 eV lower than the barrier to diffusion along the dimer rows, and hence hydrogen can diffuse extremely fast up and down the step edge at growth temperatures.

These results have important implications for our hypothesis about step-edge passivation. The dangling bond at the base of the step provides an energetically favourable site and will be

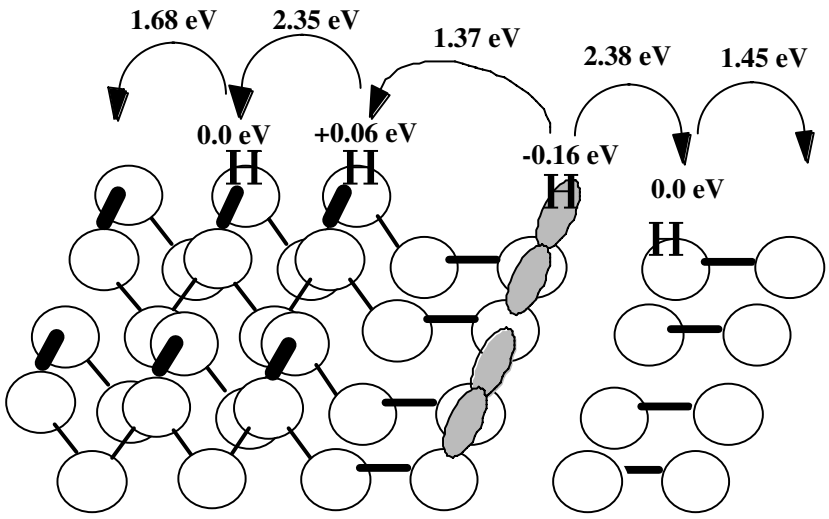

Figure 9. A schematic picture of the hydrogen adsorption sites at the base of the B-type step. Barriers are shown next to the arrows, and the relative energies of different adsorption sites are shown at the bases of the arrows. To escape from the step, the hydrogen atoms must either hop across a dimer row onto the lower terrace, or else up the step and along the dimer row at the top. Both of these routes have a barrier of $\sim$2.4 eV.

quickly saturated in the early stages of growth. This will block the adsorption of silicon dimers at the base of the step. In order to move away from the step to allow the adsorption of a silicon dimer, the hydrogen must either climb the step and diffuse away along the dimer rows on the upper terrace or else hop across a dimer row to escape onto the lower terrace. The dimer at the top of the step will be strained in a similar fashion to the dimer next to a defect, and thus the barrier to hopping off it will be similar. Both of these processes (diffusing away on the upper terrace and diffusing across a dimer row on the lower terrace) will therefore involve the surmounting of a large barrier (2.35 eV/2.38 eV respectively). Diffusion along the base of the step to a kink is possible, but will be slow compared to normal dimer row diffusion, due to the increased stability of the site next to the step edge (0.16 eV) and the crowding resulting from the increased population at the step base. Thus at growth temperatures of 650 K, the step edge is likely to remain saturated, and may be easily replenished by terrace hydrogen. This will block the adsorption of silicon dimers, and inhibit step-flow growth. Islands will nucleate, but will also be passivated before they grow to any length. The appearance of step-flow growth above 670 K is likely to be due to slow evaporation of hydrogen adsorbed at the step edge, either desorbing as H_2, or else hopping along the step edge to a kink and diffusing away along a dimer row. While hydrogen will easily hop up a step onto islands, it will probably not move beyond the first dimer, and will certainly hop back down the step rather easily. This is why the islands remain clean, as we have observed [18].

4. Conclusions

We have tested thoroughly a tight-binding parametrization for the Si(001) surface and hydrogen diffusion thereon [32]. With it, we have found barriers for all the simple diffusion modes of H on Si(001): intra-dimer hopping (1.45 eV); inter-dimer hopping (1.65 eV); paired diffusion (1.95 eV); and inter-row diffusion (2.35 eV). The error on these barriers is estimated to be 0.20 eV.

A preferential adsorption site at the step edge has been found: the dangling bond at the base of the rebonded B-type step (0.16 eV). The barrier to diffusion down the step edge has been calculated (1.37 eV). Defects act as fences with a barrier of 2.38 eV to approaching them. The top edge of a B-type step is likely to present a similar barrier. The presence of hydrogen adsorbed at the step edge which is unable to diffuse away is likely to be the cause of enhanced islanding in GS-MBE growth at 650 K.

We have shown that both DFT and the tight-binding method give calculated barriers which are in good agreement with experimental data. Moreover, the success of the computationally less expensive tight-binding method demonstrates that it may be used with confidence to calculate barriers in situations where we have no experimental data, and where the unit cell would make a DFT calculation prohibitive.

Acknowledgments

We would like to thank Henry Weinberg, Martin Castell, David Pettifor and Carl Sofield for useful discussions. JHGO and DRB were funded by the EPSRC and JHGO was also sponsored by AEA Technology, Harwell. CMG was a research fellow of Linacre College, Oxford. KM was supported by the British Council, STA (Science and Technology Agency, Japan) and the Sasakawa Foundation. Computing facilities were provided by the Materials Modelling Laboratory, Oxford (MML).

References

[1] Sinniah K, Sherman M G, Lewis L B, Weinberg W H, Yates J T Jr and Janda K C 1989 *Phys. Rev. Lett.* **62** 567
[2] Wise M L, Koehler B G, Gupta P, Coon P A and George S M 1991 *Surf. Sci.* **258** 166
[3] Boland J J 1993 *Adv. Phys.* **42** 129
[4] Lin D-S and Chen R-P 1999 *Phys. Rev.* B **60** R8461
[5] Hill E, Freelon B and Ganz E 1999 *Phys. Rev.* B **60** 15 896
[6] Swartzentruber B S 1996 *Phys. Rev. Lett.* **76** 459
[7] Krueger M, Borovsky B and Ganz E 1997 *Surf. Sci.* **385** 146
[8] Jing Z and Whitten J L 1993 *Phys. Rev.* B **48** 17 296
[9] Vittadini A, Selloni A and Casarin M 1993 *Surf. Sci. Lett.* **289** L625
[10] Wu C J, Ionova I V and Carter E A 1993 *Surf. Sci.* **295** 64
[11] Wu C J, Ionova I V and Carter E A 1994 *Phys. Rev.* B **49** 13 488
[12] Da Silva A J R, Radeke M R and Carter E A 1997 *Surf. Sci. Lett.* **381** L628
[13] Hansen U and Vogl P 1998 *Phys. Rev.* B **57** 13 295
[14] Widdra W, Yi S I, Maboudian R, Briggs G A D and Weinberg W H 1995 *Phys. Rev. Lett.* **74** 2074
[15] Vittadini A, Selloni A and Casarin M 1994 *Phys. Rev.* B **49** 11 191
[16] Voigtlander B, Weber T, Smilauer P and Wolf D E 1997 *Phys. Rev. Lett.* **78** 2164
[17] Wang Y, Bronikowski M J and Hamers R J 1994 *Surf. Sci.* **311** 64
[18] Owen J H G, Bowler D R, Goringe C M, Miki K and Briggs G A D 1997 *Surf. Sci.* **394** 91
[19] Vasek J E, Zhang Z, Salling C T and Lagally M G 1995 *Phys. Rev.* B **51** 17 207
[20] Goldfarb I, Hayden P T, Owen J H G and Briggs G A D 1997 *Phys. Rev.* B **56** 10 459
[21] Zhang J, Lees A K, Taylor A G, Xie M H, Joyce B A, Sobiesierksi Z and Westwood D I 1997 *J. Cryst. Growth* **175+176** 477
[22] Owen J H G, Bowler D R, Goringe C M, Miki K and Briggs G A D 1996 *Phys. Rev.* B **54** 14 153
[23] Bowler D R, Owen J H G, Miki K and Briggs G A D 1998 *Phys. Rev.* B **57** 8790
[24] McEllistrem M, Allgeier M and Boland J J 1998 *Science* **279** 545
[25] Chabal Y J and Raghavachari K 1984 *Phys. Rev. Lett.* **53** 282
[26] Froitzheim H, Köhler U and Lammering H 1985 *Surf. Sci.* **149** 537
[27] Hohenberg P and Kohn W 1964 *Phys. Rev.* **136** B864
[28] Kohn W and Sham L J 1965 *Phys. Rev.* **140** A1133
[29] Perdew J P and Yang W 1991 unpublished
Perdew J P 1991 *Electronic Structure of Solids '91* ed P Ziesche and H Eschrig (Berlin: Akadamie)
[30] Goringe C M, Bowler D R and Hernández E H 1997 *Rep. Prog. Phys.* **61** 1664
[31] Li P, Nunes R W and Vanderbilt D 1993 *Phys. Rev.* B **47** 10 891
[32] Bowler D R, Fearn M, Goringe C M, Horsfield A P and Pettifor D G 1998 *J. Phys.: Condens. Matter* **10** 3719
[33] Payne M C, Teter M P, Allan D C, Arias T A and Joannopoulos J D 1992 *Rev. Mod. Phys.* **64** 1045
[34] Kerker G 1980 *J. Phys. C: Solid State Phys.* **13** 189
[35] Kleinman L and Bylander D M 1982 *Phys. Rev. Lett.* **44** 1425
[36] Goringe C M 1995 *DPhil Thesis* Oxford University
[37] Owen J H G, Bowler D R, Goringe C M, Miki K and Briggs G A D 1995 *Surf. Sci. Lett.* **341** L1042
[38] More examples become apparent when the images are animated. Some of these 'movies' may be seen at http://www.math.ucla.edu/∼jhgowen/hydrogen/Hpaper.html
[39] Raschke M B and Höfer U 1999 *Phys. Rev.* B **59** 2783
[40] Pehlke E and Kratzer P 1999 *Phys. Rev.* B **59** 2790
[41] Bowler D R and Bowler M G 1998 *Phys. Rev.* B **57** 15 385